Journal Pre-proof

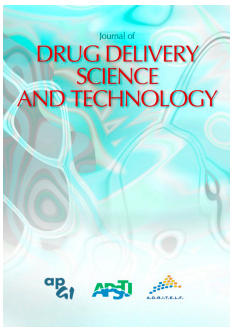

Anti-*Pseudomonas aeruginosa* phage-loaded electrosprayed lactose particles

Sai Liu, Andrew Weston, Giovanni Satta, Sara Bolognini, Mariagrazia Di Luca, Simon Gaisford, Gareth R. Williams

PII: S1773-2247(25)00254-0

DOI: https://doi.org/10.1016/j.jddst.2025.106851

Reference: JDDST 106851

To appear in: *Journal of Drug Delivery Science and Technology*

Received Date: 9 January 2025

Revised Date: 13 March 2025

Accepted Date: 22 March 2025

Please cite this article as: S. Liu, A. Weston, G. Satta, S. Bolognini, M. Di Luca, S. Gaisford, G.R. Williams, Anti-*Pseudomonas aeruginosa* phage-loaded electrosprayed lactose particles, *Journal of Drug Delivery Science and Technology*, https://doi.org/10.1016/j.jddst.2025.106851.

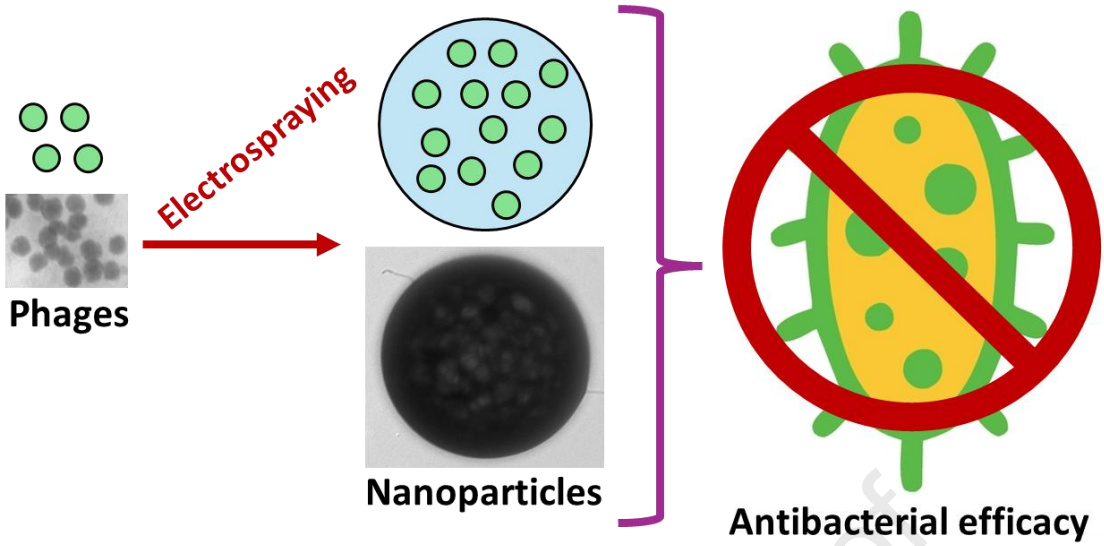

Anti-*Pseudomonas aeruginosa* phage-loaded electrosprayed lactose particles

Sai Liu[a], Andrew Weston[a], Giovanni Satta[b], Sara Bolognini,[c] Mariagrazia Di Luca[c], Simon Gaisford[a], Gareth R. Williams[a]*

[a] UCL School of Pharmacy, University College London, 29-39 Brunswick Square, London, WC1N 1AX, UK.

[b] Centre for Clinical Microbiology, University College London, Royal Free Campus, Rowland Hill Street London, NW3 2PF, UK

[c] Department of Biology, University of Pisa, Via San Zeno 39 56127 Pisa, Italy

Abstract

In light of the growing issue of antibiotic resistance, this study explored phage encapsulation within lactose particles for potential use in treating oral and ear bacterial infections. Firstly, phage-loaded suspensions that ensured phage stability at RT for 24 h were developed. After electrospraying, phage-loaded particles were successfully generated with an encapsulation efficiency (EE) of 31% at a phage stock concentration of 50% v/v. The phage titer decreased only slightly from 5×10^7 PFU/mg to 1.5×10^7 PFU/mg after processing, maintaining the same order of magnitude. The particles exhibited spherical morphology and successful phage encapsulation, with a burst release of phages within 10 minutes of immersion in an aqueous medium (99.0 ± 6.9%). The phage-loaded particles demonstrated enhanced antibacterial efficacy compared to pure phage solutions, completely inhibiting *P. aeruginosa* growth for over 24 h at a particle concentration of 20 mg/ml, likely due to a high localized phage concentration. Stability studies indicated that phages remained viable at various temperatures, with greater stability at lower temperatures (4°C, and -20°C), though phage activity gradually decreased over time in particle form, particularly at room temperature.

1. Introduction

Oral and outer ear bacterial infections are significant concerns, in part due to their association with respiratory diseases [1,2]. There is a strong correlation between bacterial respiratory infections and the ear infection otitis media, with otitis media patients having a significantly higher likelihood of bacterial lung infections [3,4]. Similarly, oral bacterial infections have been linked to an increased risk of multiple respiratory diseases [5]. For example, a study among the elderly Japanese population found that adjusted mortality due to pneumonia was 3.9 times higher in individuals with periodontal disease [6].

Antibiotics are commonly used for the treatment of oral and outer ear bacterial infections [7,8]. However, the emergence of multi-drug-resistant bacteria complicates antibiotic treatments [9]. In this context, phage therapy has emerged as a promising alternative for treating bacterial infections in the mouth and outer ear [10,11]. Phages, which are viruses lacking metabolic activity, exhibit antibacterial effects by deploying lytic enzymes to dismantle specific bacteria following their attachment to the bacterial surface, penetration, and subsequent replication within the bacterial host [12].

In contrast to antibiotics, phages offer a natural, low-toxicity alternative that is self-amplifying, highly specific, and adaptable. They are thus capable of circumventing bacterial resistance [13]. Their ability to target infected bacteria specifically, along with their established clinical safety and self-replicating capacity, positions phages as promising, safe, and resilient antimicrobial agents for the future. Numerous studies have validated the efficacy and safety of phage therapy. For instance, two environmental phages PA5oct and KT28 [14], φNH-4 and φMR299-2 [15] have demonstrated *in vitro* antibacterial activity against drug-resistant *P. aeruginosa*. Additionally, animal studies have showcased the effectiveness of phage therapy [16,17]. Crucially, human trials

have reported promising therapeutic outcomes in the treatment of drug-resistant respiratory infections, with success rates of up to 60% observed across various studies [18-20]. The utilization of phage cocktails, comprising multiple phage species, allows the treatment of multiple bacterial strains simultaneously [21-23].

Most phage preparations are formulated as liquids [24] with salts, gelatin, and buffered media used to enhance phage stability [25]. However, solid formulations are often preferred for transport, patient convenience, and ease of administration. To this end, methods such as lyophilization, spray drying, electrospinning, and electrospraying have been employed to convert phage suspensions into dry formulations [26]. Among these, electrospraying stands out for its ease, cost-effectiveness, and scalability [27].

Electrospraying functions by dispersing a liquid into droplets using electrical forces [28] (**Figure 1**). In this process, a solution is dispensed at a controlled rate from a narrow-bore needle (the spinneret). When a droplet is expelled from the end of the spinneret, upon the application of an electric field it assumes a cone shape and eventually the electrostatic force surpasses the surface tension and a jet ejects, leading to the break-up of the droplet into smaller charged droplets. These then undergo solvent evaporation to yield solid products comprising nano-microscale particles [29].

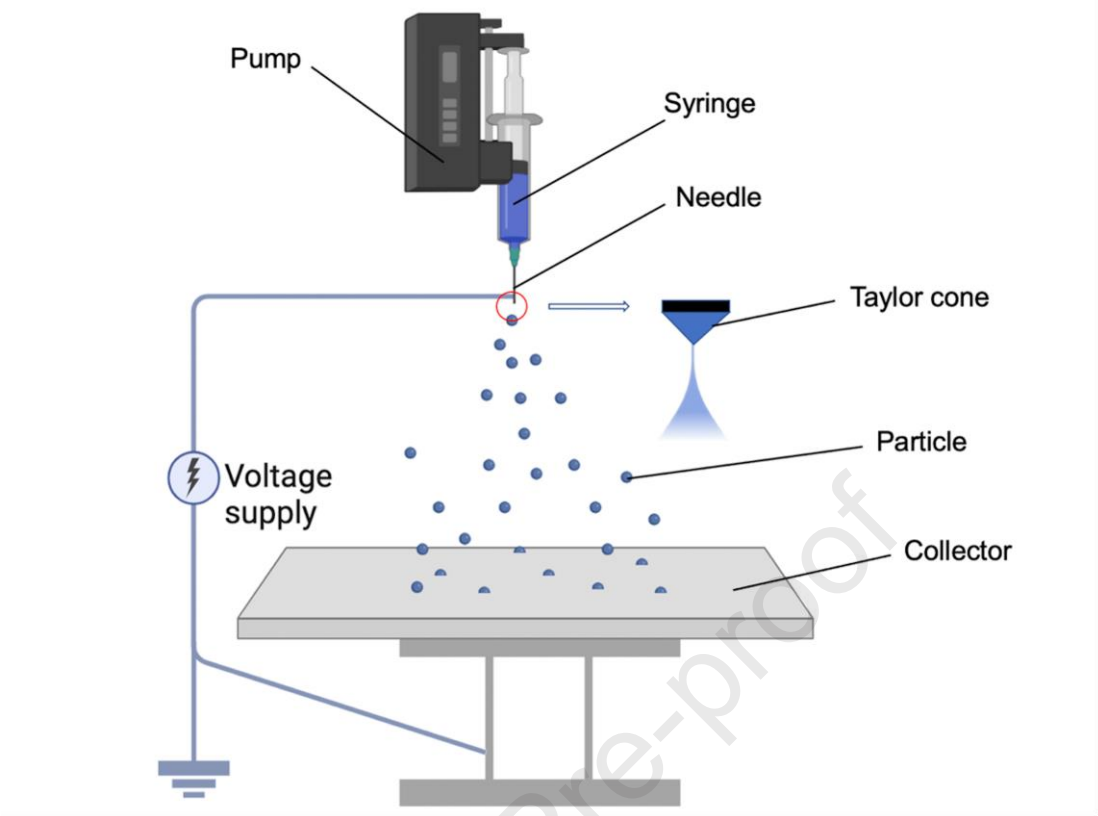

Figure 1 Schematic diagram of the electrospraying set up (drawn in BioRender).

Electrospraying offers the capability to produce particles with uniform size distributions and consistent morphologies through precise control of process parameters [30]. A fundamental requirement is establishing a stable cone-jet mode, achievable by fine-tuning parameters such as voltage, solution conductivity, and flow rate [31]. Additionally, particle morphology and size can be further regulated by adjusting parameters like polymer concentration, molecular weight, voltage, solvent vapor pressure, flow rate, and collection distance [32]. The environmental conditions, including relative humidity and temperature, also influence the electrospraying process and the properties of the resultant particles [33].

There have been a few studies on electrosprayed phage-loaded particles [34-37]. Compared to conventional nebulization, electrospraying generates cleaner, more stable, and more viable MS2 phage-loaded particles [35] with a narrow

size distribution [36]. Additionally, electrosprayed particles were found to give lower Felix O1 phage activity loss in simulated gastric fluid compared to those produced via freeze drying [37]. Moreover, ES particles have also shown great promise in combating bacterial infections in the mouth and ear [38-41].

The objective of this study is to develop phage-loaded lactose particles to combat oral/outer ear bacterial infections. Polyvinyl alcohol (PVA) was incorporated to enhance the viscosity of the lactose solution, ensuring stable electrospray formation. Given that *P. aeruginosa* is a primary pathogen in these infections, an anti- *P. aeruginosa* phage was selected. A suitable formulation matrix to ensure phage stability was first developed. Next, phage-loaded particles were generated by electrospraying and the phage loading maximised. The phage-loaded formulations were fully characterised in terms of their morphology, physicochemical properties, phage loading efficiency, phage release kinetics, antibacterial activity, and stability.

2. Materials and methods

2.1 Materials

Materials were obtained as follows: poly (vinyl alcohol) (PVA, MW 30,000 Da, Merck); lactose monohydrate (LM, $C_{12}H_{22}O_{11}\cdot H_2O$, MW 360.30 g/mol, Fisher Scientific); phosphate buffered saline (PBS) tablets (Sigma-Aldrich); glycerol (Fisher Scientific); Tryptic Soy Agar (TSA, Sigma-Aldrich); Tryptic Soy Broth (TSB, Sigma-Aldrich); Mueller Hinton Agar (MHA, Sigma-Aldrich); Tris·HCl (EMD Millipore Corp.); NaCl (Fisher Scientific); $MgSO_4\cdot 7H_2O$ (Thermo Fisher Scientific); gelatin (Sigma-Aldrich); *Pseudomonas aeruginosa* (NCTC 12903, TCS Biosciences); *Pseudomonas aeruginosa* phage Neko (10^{12} PFU/ml), isolated from a puddle water in La Spezia, Italy; SM buffer (50 mM Tris-HCl, 0.1 M NaCl, 8 mM $MgSO_4.7H_2O$, 0.01% w/v gelatin, pH 7.5); Triton-X100 (Thermo Scientific); deionized water (Purite, Triple Red Limited); phosphotungstic acid

(PTA, Sigma-Aldrich); potassium hydroxide (KOH, Fisher Scientific); TEM grids (3.05 mm copper grid formvar/carbon support film 300 mesh, TAAB Laboratories Equipment Limited).

2.2 Bacterial culture

Initially, a bacteria pellet (*P. aeruginosa* NCTC 12903) was dispersed and vortexed in 1 ml of TSB (first generation), which was then transferred to and grown in 40 ml TSB in an incubator (37 °C) for 24 h. Following incubation, the resultant culture was vortexed, and 1 ml of the culture was transferred to 40 ml of fresh TSB for subculture (second generation). After subculture for two generations (always vortexing before subculture), 5 ml of the overnight culture from the last generation was added to 250 ml of fresh TSB broth and incubated at 37 °C. A 1 ml sample of the culture suspension was withdrawn, vortexed, and its optical density (OD) measured at a wavelength of 600 nm using a spectrophotometer (CO8000 cell density meter, WPA Biowave). Once the OD reading fell between 0.4 and 0.7, indicating the bacteria were in the exponential growth phase, the culture was processed for freezing.

In this processing, 0.1 ml of culture suspension was transferred into sterile tubes with 0.9 ml of PBS and labeled as 10^{-1}. This solution was then serially diluted tenfold to obtain dilutions from 10^{-2} to 10^{-7}. Subsequently, 50 µl from each dilution was inoculated onto TSA plates and spread with a fresh L-shaped hockey spreader. After 24 hours of incubation, plates containing a countable number of colonies (ranging from 2 to 300 colonies) were selected, and the colonies were counted to establish colony-forming units per milliliter (CFU/ml) for each dilution, in triplicate. The final dilution factor chosen to count was 10^{-5} (10^{-1}-10^{-4} had too many colonies). After counting the colonies in the 10^{-5} plates, the final inoculum calculated was 10^{8} CFU/ml.

The remaining liquid culture, with OD between 0.4-0.7, was centrifuged at 9500 rpm at 4°C for 10 mins, resulting in a pellet. Then the supernatant was discarded, and the tubes were refilled with PBS, in which the pellet was re-suspended and centrifuged. The PBS re-suspension and centrifugation processes were repeated 3 times. Finally, the pellet was resuspended in 20% glycerol, transferred into 2 ml cryovials and frozen at -80 °C. For each step, vortexing was necessary and TSA plates were prepared for streaking to ensure purity control (without signs of contamination).

2.3 Phage harvesting and plaque assay

The methods for phage harvesting and plaque assay were adapted from a previous study [36]. Initially, 100 µl of *P. aeruginosa* was inoculated into 5 ml of TSB media and incubated overnight at 37 °C. From this culture, a 1 ml sample was taken, and its optical density (OD) was measured at 600 nm using a spectrophotometer (CO8000 cell density meter, WPA Biowave). Once the OD reading was between 0.5 and 0.6 (indicating the exponential phase), a 100 µl aliquot of the overnight culture was then mixed with 100 µl of phage stock solution. This mixture was incubated at 37°C for 30 min, mixed with 4 ml of partially cooled 2% w/v MHA, then poured onto a cooled MHA plate and incubated at 37 °C overnight. Phage growth manifested as a clear, transparent plate compared to the cloudy control plate (containing 100 µl of *P. aeruginosa*). To recover the phages, 4 ml of SM buffer was added to the plates and incubated at 4 °C for 1 h. The SM buffer containing phages and 2% w/v MHA was then centrifuged at 6500 rpm for 30 min at 4°C. The supernatant was filtered through a 0.22 µm sterile filter and stored at 4°C. The lytic activity of the phages was assessed using a plaque assay.

For the plaque assay, serial dilutions of the harvested phages were prepared. Aliquots of 100 µl from each dilution were mixed with an equal volume of *P. aeruginosa* host culture (OD: 0.5-0.6). Each mixture was incubated at 37 °C for

30 min, mixed with 4 ml of partially cooled 2% w/v MHA, poured onto an MHA plate, and incubated overnight at 37 °C. A negative control, consisting of *P. aeruginosa* host without phages, was prepared in the same manner. Following overnight incubation, plates containing a countable number of plaques (2-300) were selected, and the plaques were counted to establish plaque forming units per milliliter (PFU/ml) for each dilution, in triplicate. Phage titer was determined to be 10^{10} PFU/ml.

2.4 Phage stability in the formulation solution

Before electrospraying, the stability of the phages in formulation solutions was evaluated at room temperature (RT) over 24 hours. Phage viability was assessed using a plaque assay. The negative control was *P. aeruginosa* host without phages, while phage stock alone comprised a positive control. The final solvent system chosen was SM buffer with 0.1% Triton-X-100 (v/v). Two specific formulations were tested: one with 20% v/v phage stock in SM buffer containing 0.1% Triton-X-100 (S_0), and 20% v/v phage stock with 40% w/v LM and PVA in a 9:1 ratio (w/w) in SM buffer with 0.1% Triton-X-100 (F_0). The phage titer was measured at predetermined intervals (10 min, 1 h, 24 h) using the plaque assay method. All tests were conducted in triplicate.

2.5 Preparation of electrospraying solutions

After confirming the stability of the phages in the formulation solution, the electrospraying solutions were prepared. Initially, LM and PVA were dissolved in the solvent blend at 130 °C and then allowed to cool to room temperature. The cultured phage stock solution was then added and thoroughly vortexed to ensure complete mixing before electrospraying. Once the formulation was confirmed to be suitable for electrospraying, the focus shifted to achieving the highest possible phage loading. The final formulation consisted of 40% w/v solute (LM: PVA= 9:1 w/w) in SM buffer with 0.1% Triton-X-100 (v/v), with a

final phage concentration of 50% v/v (50% v/v phage suspension in the final liquid formulation) (F_1).

2.6 Production of phage-loaded ES particles

The solutions were electrosprayed using a 1 ml syringe (BD Plastipak) equipped with a 20G needle (0.337 mm inner diameter, Nordson EFD). The distance between the needle tip and the collector was set to 20 cm. The flow rate was maintained at 0.01 ml/h. A voltage of 20 kV was applied for both the blank and phage-loaded formulations. The electrospraying process was conducted in a temperature range of 20-25°C, with relative humidity maintained between 25% and 40%.

2.7 Transmission electron microscopy (TEM)

TEM was utilized to examine the morphology of the phages and phage-loaded particles. The phage sample was prepared by staining with a filtered 2% w/v phosphotungstic acid (PTA) solution (pH=7, neutralized using a 2 M KOH solution) on a carbon film-coated copper grid. For the phage-loaded particles, the specimens were prepared by directly depositing the electrosprayed particles onto a carbon film-coated copper grid for 10 seconds, without staining.

2.8 Scanning electron microscopy (SEM)

SEM (Phenom Pro microscope, Thermo Fisher Scientific) was employed to study the morphology of the particles. SEM images of the particles were collected after being sputter coated with graphite. Then, for each formulation, 200 particles from different images were selected and analyzed with the ImageJ 1.52a software. The size results are presented as mean ± standard deviation. Size distributions were plotted using Origin 2022b (OriginLab Corporation).

2.9 X-ray diffraction (XRD)

A Rigaku Miniflex 600 diffractometer supplied with Cu Kα radiation (λ = 1.5418 Å) was used for XRD measurements, performed at 40 kV and 15 mA with 2θ ranging from 3° to 40° (at 5°/min).

2.10 Fourier-transform infrared spectroscopy (FTIR)

A PerkinElmer Spectrum 100 FTIR spectrometer was used to collect spectra (four scans) in attenuated total reflectance mode, within the range of 4000-650 cm^{-1} at a resolution of 1 cm^{-1}.

2.11 Phage lytic activity after electrospraying

Phage-loaded particles were suspended in 0.5 ml of SM buffer and incubated overnight at 37 °C with continuous shaking. The resulting solution was then subjected to serial dilutions. The phage lytic activity was evaluated using a plaque assay to determine the PFU/ml. A negative control consisted of *P. aeruginosa* host without phages. Finally, the plaque forming units per milligram (PFU/mg) was calculated. The phage encapsulation efficiency (EE, %) was determined according to the equation:

EE (%) = (calculated PFU/mg) / (theoretical PFU/mg) × 100% (1)

The results are reported as mean ± standard deviation (SD). All experiments were conducted in triplicate.

2.12 Phage release

Phage-loaded particles were suspended in 5 ml of SM buffer and incubated at 37 °C with shaking at 50 rpm. At predetermined intervals over a 24-hour period, 10 µl of the release medium was sampled and replaced with an equal volume of preheated fresh SM buffer. Serial dilutions of the samples were prepared to

assess phage lytic activity using a plaque assay, determining the PFU/ml. A negative control included *P. aeruginosa* host without phages. The results are presented as a cumulative release (%) versus time (min) curve. All experiments were conducted in triplicate.

2.13 Antibacterial tests

The antibacterial activities of phage and phage loaded particles against *P. aeruginosa* were conducted *in vitro* using isothermal microcalorimetry.

2.13.1 Antibacterial activity of phages

Serial dilutions of the phage stock solution were prepared using SM buffer. In a 3 ml calorimetric glass ampoule, 2 ml of pre-warmed TSB (37°C), varying concentrations of the phage stock solution (0.03 ml), and sterile water (0.94 ml) were combined. Following this, 0.03 ml of bacterial culture was added, bringing the total volume to 3 ml. The ampoule was sealed, vortexed, and placed in a Thermal Activity Monitor (TAM; TA Instruments Ltd.), where it equilibrated for 30 minutes at 37 °C. Data collection was performed using the Digitam 4.1 software, with an amplifier setting of 3000 µW. Control groups included pure bacteria, and phages (10^8 PFU/ml) without bacteria. Each concentration was tested at least three times, and the resulting curves were consistent, so one representative dataset is reported. The isothermal microcalorimetry results are presented as heat flow (µW) vs. time (h). The bacterial inoculation size was 10^6 CFU/ml. After the TAM run, the ampoule was unsealed, and the sample solution was diluted to determine CFU/ml and PFU/ml.

2.13.2 Antibacterial activity of phage-loaded particles

The *in vitro* antibacterial activity of phage loaded particles against *P. aeruginosa* was also evaluated by TAM. Various concentrations of the blank formulation and phage-loaded particles were prepared. In each ampoule, 2 ml of pre-

warmed TSB (37 °C), 0.03 ml of bacterial inoculum, the sample, and water were combined to make a total volume of 3 ml. The ampoules were then loaded into the TAM. Control groups included pure bacteria and the blank formulation. Four concentrations of the phage-loaded formulation were tested, at least in triplicate. The resulting heat flow curves were consistent, so one representative dataset is shown. The bacterial inoculation size was 10^6 CFU/ml. After the TAM run, the ampoule was unsealed, and the sample solution was diluted for testing CFU/ml and PFU/ml.

2.14 Stability tests

A freshly cultured phage stock solution was vortexed and divided into three aliquots to assess phage stability at RT, 4°C, and -20 °C over a 2-month period. Additionally, freshly prepared phage-loaded particles from the same batch of phage stock solution were stored under the same conditions. For the phage stock solution, the lytic activity of the phages at different time points was evaluated using the plaque assay test. At various time points, the phage-loaded particles were suspended in 0.5 ml of SM buffer and incubated overnight at 37 °C with gentle shaking. Following this incubation, serial dilutions of the resulting solution were prepared to evaluate phage lytic activity using a plaque assay, which allowed for the determination of PFU/ml. The experiments were performed in triplicate, and PFU/mg was subsequently calculated.

3. Results and discussion

3.1 Phage characterization

Figure 2 shows TEM images of the Neko phages. Neko is a Podovirus, belonging to the *Caudoviricetes* family which was characterized in a previous work [42].

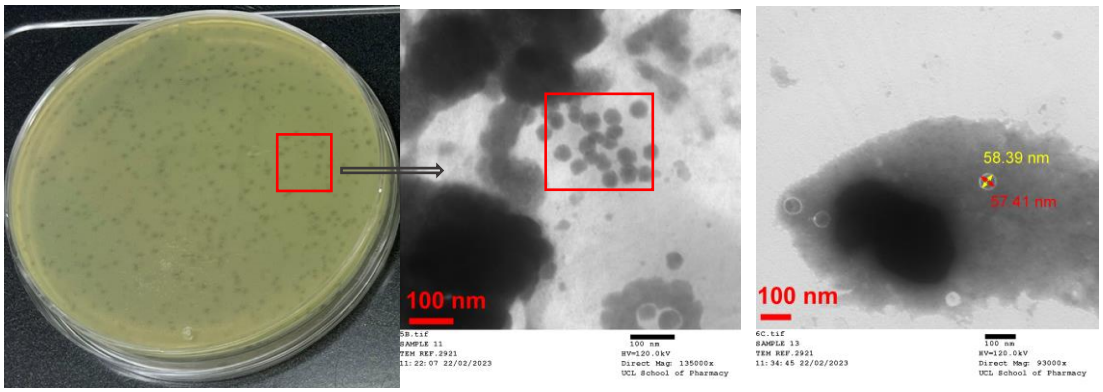

Figure 2 Morphology of plaques on double-layer agar plate **(left)** and TEM images of *P. aeruginosa* NCTC 12903 targeting phages **(middle and right)**.

3.2 Optimizing solvent systems

It was found that the phage titers remained consistent up to 24 h when the stock was held at RT (Supporting Information, **Figure S1**). The phages were next mixed with SM buffer or with SM buffer augmented with Triton X-100, LM, and PVA. Phage stability was found to be maintained in these conditions (**Figure S2**), and thus a solvent system of 20% v/v phage suspension, 40% w/v, LM: PVA=9:1 w/w, SM buffer and 0.1% (v/v) Triton-X-100) (F_0) was selected for onward experiments.

3.3 Generation of electrosprayed particles

Both the blank formulation (without phages) and F_0 yield particles with uniform spherical morphology (**Figure 3a,b**). After electrospraying however, the phage titer reduced from 1.6×10^7 PFU/mg to 6.2×10^5 PFU/mg. The final encapsulation efficiency was also low, at 3.8 ± 0.7 %. This was felt to be too low, and therefore the phage stock concentration was increased to 50% v/v in further experiments. This gave formulation F_1, which comprised 50 % v/v phage stock, 40% w/v LM: PVA=9:1 w/w, SM buffer, and 0.1% v/v Triton-X-100. F_1 also produced particles with spherical morphology (**Figure 3c**), though a few larger particles were also observed. A possible reason for this might be the uneven mixing of the phage suspension and formulation solution or spray

instability during the electrospraying process [34]. With F_1 the phage viability remained more consistent, ranging from $5x10^7$ PFU/mg to 1.5 $x10^7$ PFU/mg. The EE of F_1 was 31 ± 8 %, again a notable improvement on the F_0 system.

The particle sizes were found to be 1.8 ± 0.9 µm (blank), 2.9 ± 1.1 µm (F_0), and 1.4 ± 0.7 µm (F_1). A low loading of phages thus has little impact on the overall particle size, while with the higher-loading F_1 formulation the particle size is somewhat increased. This finding is aligned with the literature [43]. Considering the size distribution (**Figure 3d**), F_1 exhibited the narrowest size distribution. This implies that at this high concentration, the phages may function as stabilizers or regulators. They could potentially reduce particle aggregation or clumping, helping to keep more small particles dispersed and resulting in a more uniform particle size distribution.

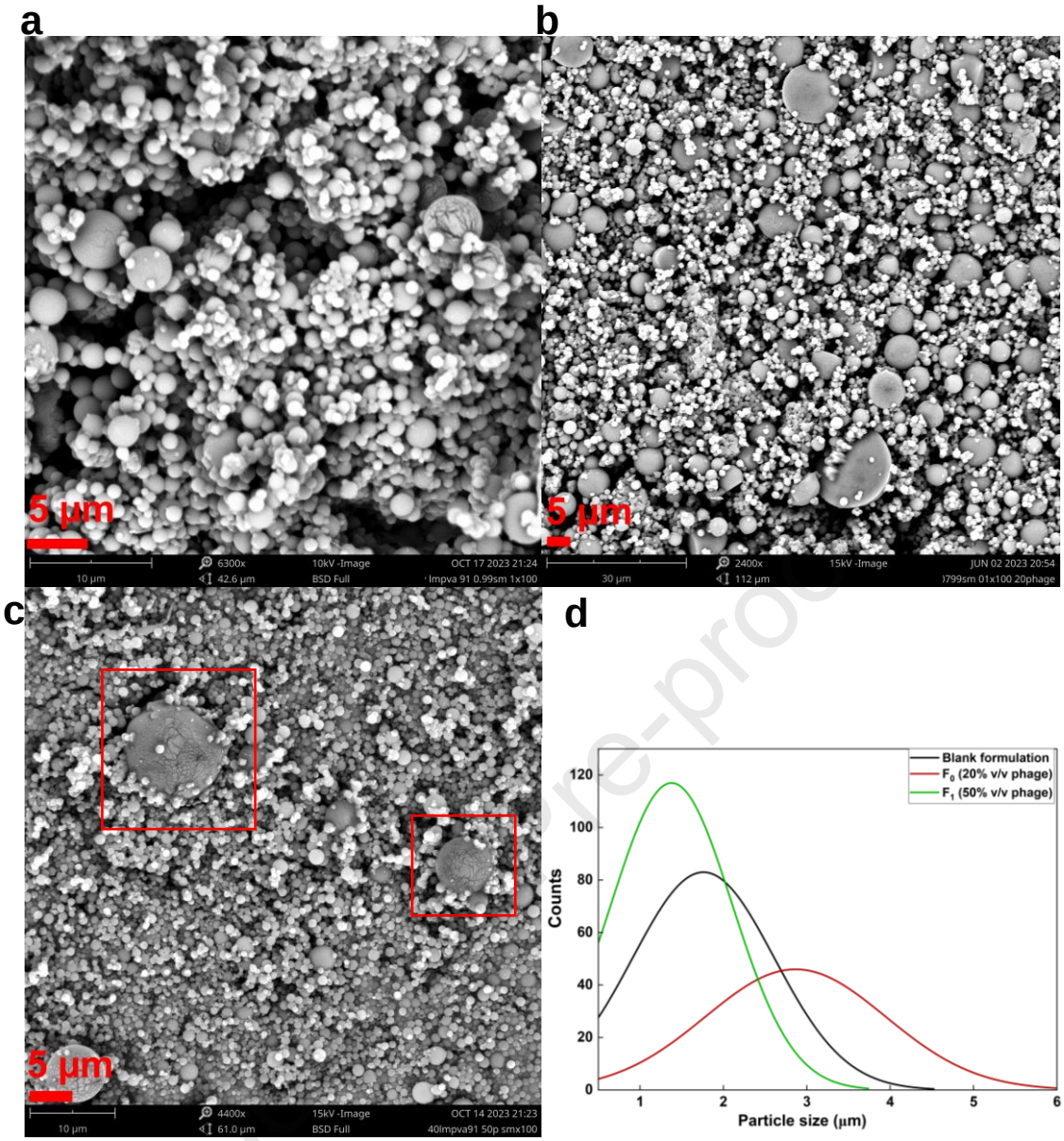

Figure 3 SEM images of **(a)** the blank formulation (40% w/v, LM: PVA=9:1 w/w, SM buffer+ 0.1% (v/v) Triton-X-100), **(b)** F_0, **(c)** F_1 with **(d)** the size distribution curves.

3.4 F_1 characterization

Figure 4 displays TEM images of the electrosprayed particles. The blank particles (**Figure 4a**) and phage loaded F_0 particles (**Figure 4b**) reveal no internal structures (possibly due to the low phage encapsulation efficiency), whereas encapsulated phages are clearly visible within the phage-loaded F_1 particles (**Figure 4c-d)**). This is in agreement with previously reported studies [43,44]. The TEM images highlight a non-uniform distribution of phages within

the particles. **Figure 4c** and **Figure 4d** illustrate that some particles contain a high density of phages, while others have fewer. This may be attributed to factors such as variations in the evaporation rate of the solution, particle shrinkage and solidification, and interactions between the phages and other solutes [45].

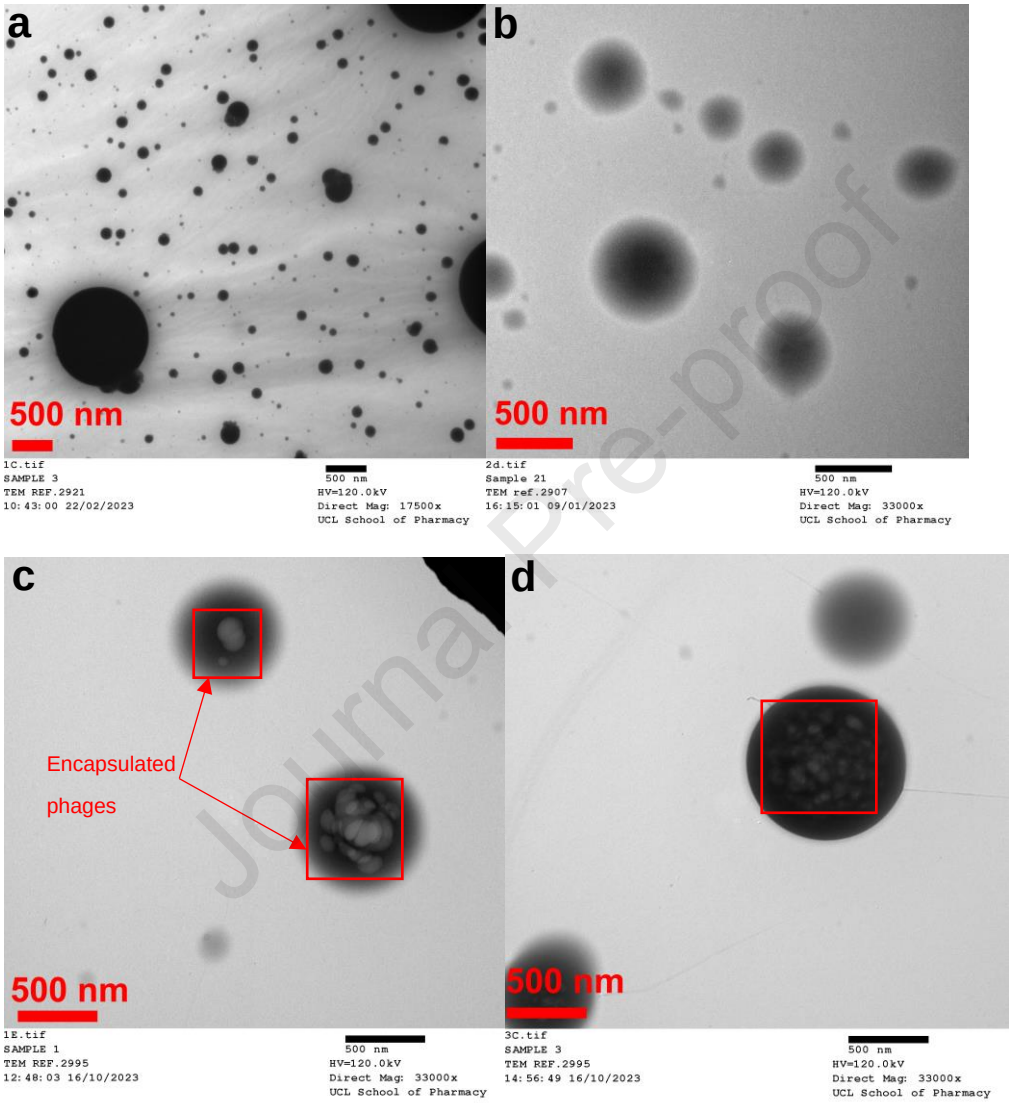

Figure 4 TEM images of **(a)** blank formulation, **(b)** F_0 and **(c-d)** F_1.

XRD patterns (**Figure S3**) of the blank and F_1 formulations show both to be amorphous systems, with no crystalline LM present. FTIR spectra are displayed in **Figure S4**. The IR data show no distinct differences between the blank and F_1 spectra, presumably because the functional groups present in the phages overlap with those in the excipients, and the latter dominate the spectrum.

3.5 Phage release

The phage release experiment tracked the phage release profile of F_1 over a 24 h period (see **Figure S5**). F_1 gives a burst release of phages within the first minute, and almost complete release (99.0 ± 6.9%) within 10 minutes (**Figure 5**). A set of photos demonstrating plaque assay results for the released phages reveals that the number of released phages remains constant over 24 h (see **Figure S6**). This burst release might be attributed to the rapid dissolution of lactose and PVA in the aqueous buffer.

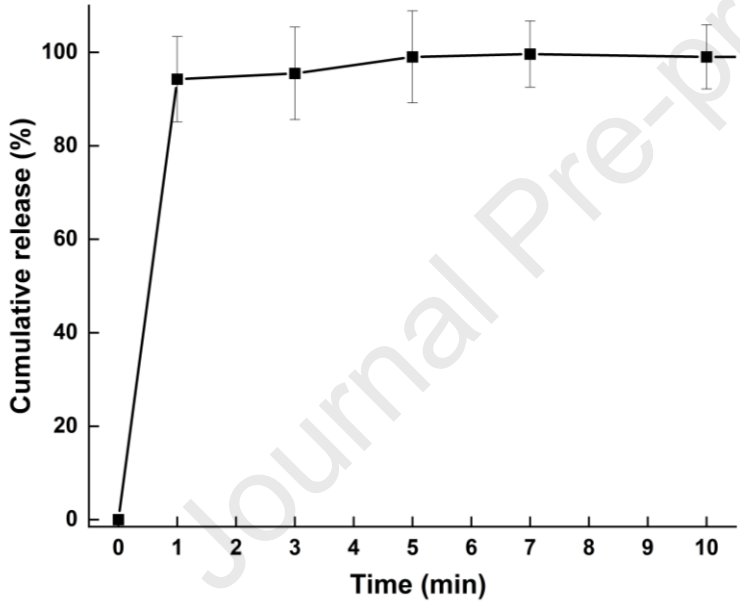

Figure 5 An enlarged view of the first 10 min of the release profile of F_1 (mean ± SD, n=3)

3.6 Antibacterial activity of phages

The antibacterial effect of the phages against *P. aeruginosa* was investigated by isothermal microcalorimetry (**Figure 6a**). Isothermal microcalorimetry was employed to measure heat flow and thereby obtain insight into bacterial and phage interactions, providing metabolic insights that go beyond what can be seen in plaque assays [46]. While plaque assays quantify bacterial killing, isothermal microcalorimetry enables real-time monitoring of dynamic metabolic

responses, offering a more detailed view of activity [47]. Compared to traditional static methods like broth dilution, it is time-resolved, highly sensitive, quantitative, and non-invasive, capable of detecting subtle changes in bacterial activity [48]. Additionally, it can assess both inhibitory and bactericidal effects, [49].

The complex growth curve reflects organism growth in an oxygen-limited medium (the sealed ampoule restricts oxygen to what is dissolved in the medium and present in the headspace). Initially, the exponential phase represents aerobic metabolism (first peak), followed by a transition to anaerobic metabolism at around 5 hours, initiating a second exponential growth phase (second peak) [50]. Successive peaks and troughs suggest the sequential utilization of major nutrients in the medium. However, as nutrients are depleted or environmental conditions worsen due to metabolite accumulation, the heat-producing reactions cease, causing the power signal to return to baseline [50].

The pure phage sample (red line) shows no heat output. Compared to the control groups—pure bacteria without phages (GC) and pure phages without bacteria— *P. aeruginosa* incubated with varying concentrations of phages exhibits concentration-dependent delayed bacterial growth and reduced peak height (indicative of fewer bacteria). This is consistent with the antibacterial activity of the phages. This finding is further supported by CFU/ml and PFU/ml measurements taken after TAM, as presented in **Figure 6b**. The data confirm that a concentration of 10^8 PFU/ml has the strongest antibacterial effect, yielding the lowest CFU/ml ($2.1 \times 10^7 \pm 0.5 \times 10^7$).

After incubation with the bacterial host, initial phage concentrations (C_i) from 10^2 to 10^7 PFU/ml lead to notably greater final phage titers (C_f), which are increased by at least an order of magnitude. When $C_i = 10^8$ PFU/ml concentration, C_f shows a two-fold increase (**Figure 6b**). This phenomenon can

be attributed to the replication of phages within the bacterial host [51]. After infecting the bacteria, the phages utilize the bacterial replication machinery to produce new phage particles, leading to a rapid increase in phage numbers [51]. However, although there is a noticeable reduction in bacterial count, even at the highest concentration tested (10^8 PFU/ml) complete bacterial inhibition cannot be achieved.

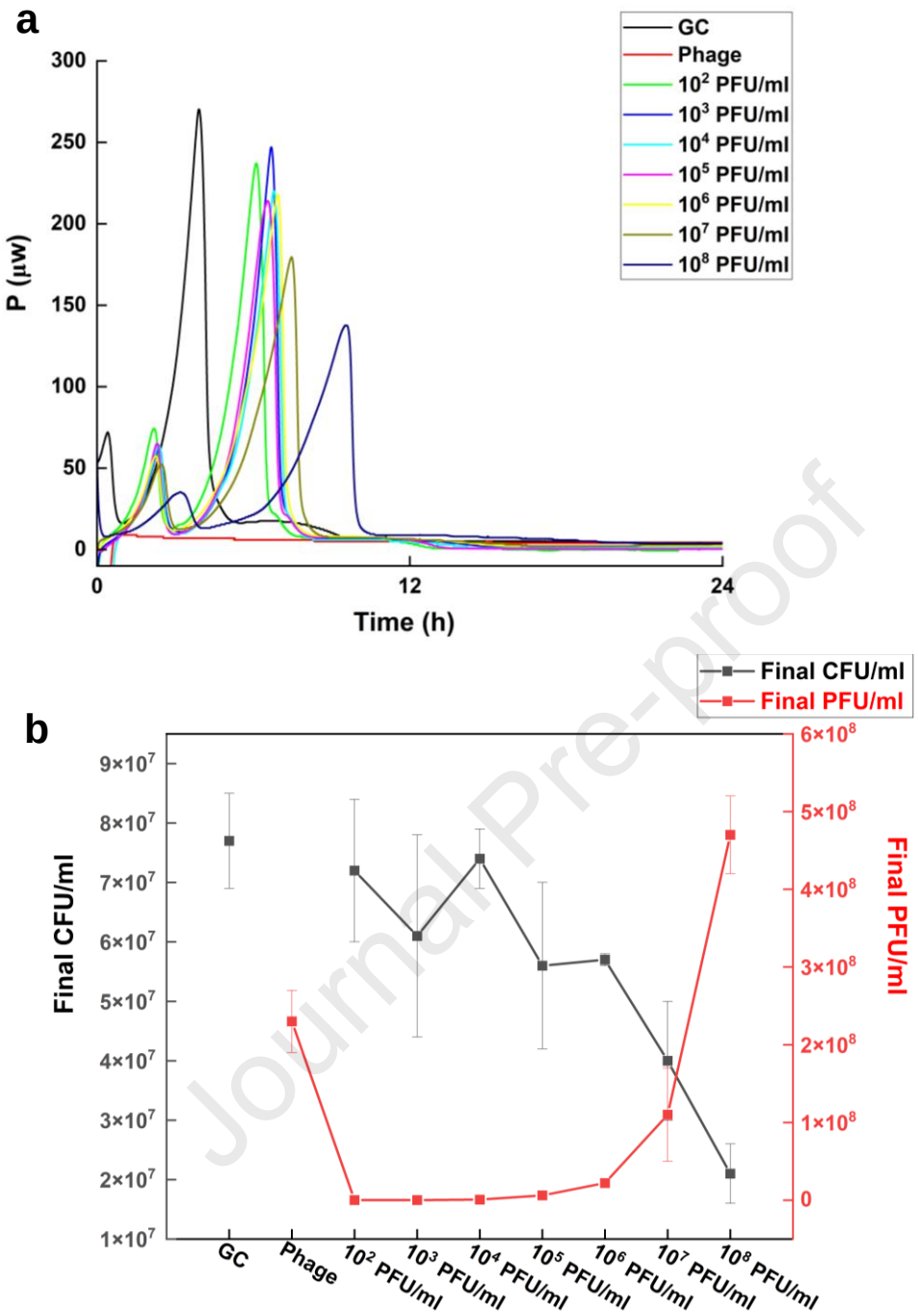

Figure 6 (a) Heat flow (μW) vs time curves of *P. aeruginosa* incubated with different concentrations of phages for 24h (GC: negative control; phage: positive control, phage concentration was 10^8 PFU/ml). The inoculation of bacteria was 10^6 CFU/m; **(b)** *P. aeruginosa* final CFU/ml and final phage PFU/ml trend curves after incubation with different phage concentrations for 24 h.

These results suggest that while the phages can infect and reduce the bacterial population in a liquid environment, they are unable to completely inhibit bacterial growth, even at high concentrations. This highlights the importance of using phage cocktails, which combine multiple phages to improve antibacterial efficacy [52].

3.7 Antibacterial activity of phage-loaded particles

Figure 7a and **Figure 7b** illustrate the heat flow curves of different concentrations of blank particles against *P. aeruginosa*. The *P. aeruginosa* used in this study (NCTC 12903) responds to the blank formulation, characterized by a higher peak height indicating an increased bacterial count. This observation is further supported by the final bacterial count (CFU/ml) after exposure to different concentrations of the blank formulation (the initial bacteria concentration is 10^6 CFU/ml) (**Figure 7c**). The blank particles appear to provide nutrients (lactose) to the bacterial host, as the bacterial count increases to 10^8 CFU/ml compared to the GC (10^7 CFU/ml).

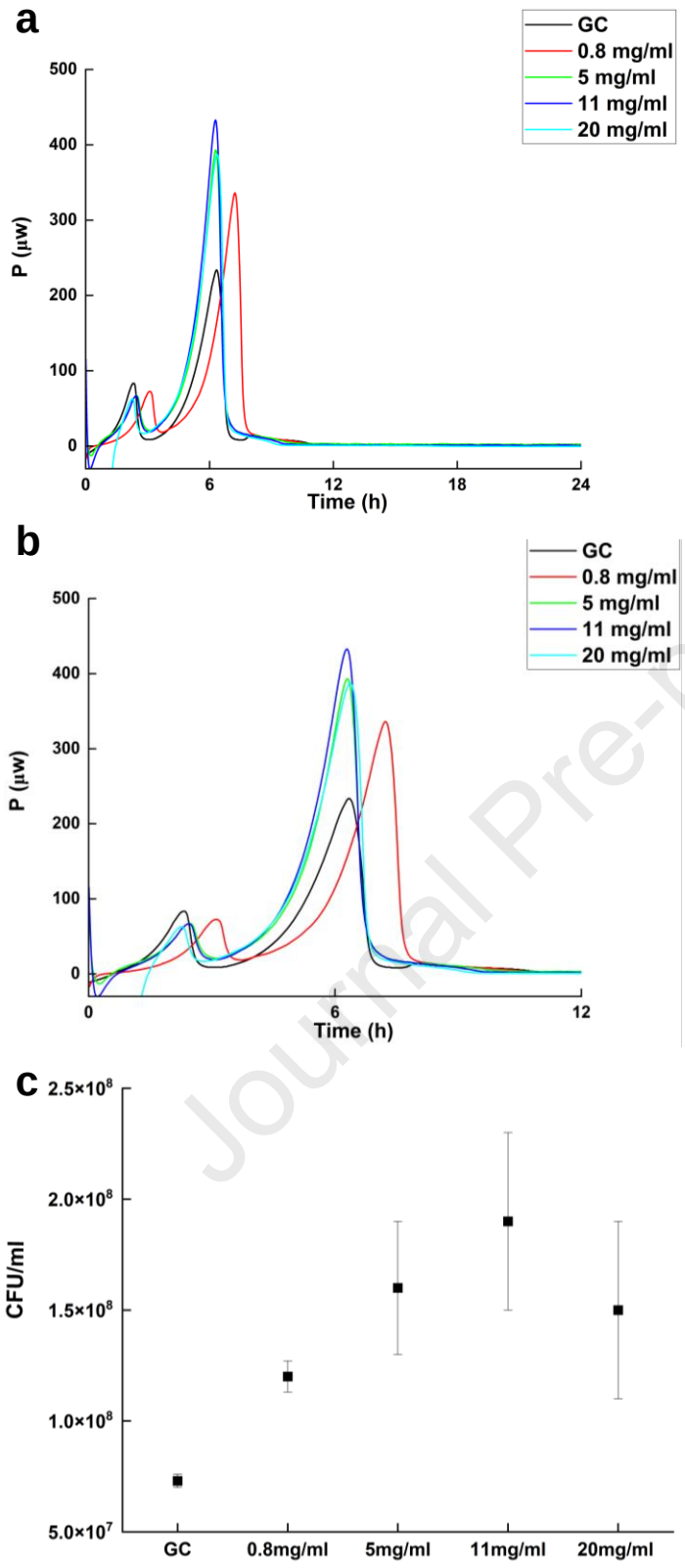

Figure 7 (a) Heat flow (µW) vs time curves of *P. aeruginosa* incubated with different concentrations of the blank formulation. **(b)** Enlarged view over the first 12 h. Inoculum of bacteria was 10^6 CFU/ml. **(c)** Final CFU/ml of bacteria exposed to the blank formulation for 24 h.

For F_1 (**Figure 8a**), at a concentration of 0.8 mg/ml, the antibacterial effect of the incorporated phages ultimately controls the bacterial count at the same level as the GC group (10^7 CFU/ml) despite the pro-growth effects of the matrix materials. When the particle concentration was increased to 5 mg/ml, the bacterial count further decreases compared to the 0.8 mg/ml and GC groups, due to the higher phage content (enhanced antibacterial activity), but still remains at 10^7 CFU/ml (**Figure 8b**). At 11 mg/ml, the antibacterial effect becomes more pronounced, delaying bacterial growth by up to 18 h (**Figure 8a**). At a concentration of 20 mg/ml, no bacterial growth is seen for at least 30 h, indicating that the minimum heat inhibition concentration (MHIC) of F_1 particles is 20 mg/ml.

As demonstrated by **Figure 8b**, compared with control groups (GC and blank), increased F_1 particle concentrations lead to decreased final bacteria concentrations and increased final phage numbers. Even though the 10^8 PFU/ml phage suspension (4×10^8 PFU/ml) had a slightly higher intial titer than the 20 mg/ml suspension of F_1 particles (3×10^8 PFU/ml), both reached a final titer of 4.7×10^8 PFU/ml (**Figure 6b, Figure 8b**). This demonstrates that the encapsulation process did not significantly affect phage activity [26,37]. Moreover, the F_1 particles were more effective in inhibiting bacterial growth. This might be a result of local high-concentration effects, where the particles create a high local concentration of phages, increasing the contact and infection rates between phages and bacteria [53]. Also, the materials in the particles (such as Triton X-100) may alter the properties of the local environment, making it easier for phages to infect bacteria. These materials may change the structure or permeability of bacterial cell membranes [54], thereby increasing the infection efficiency of phages.

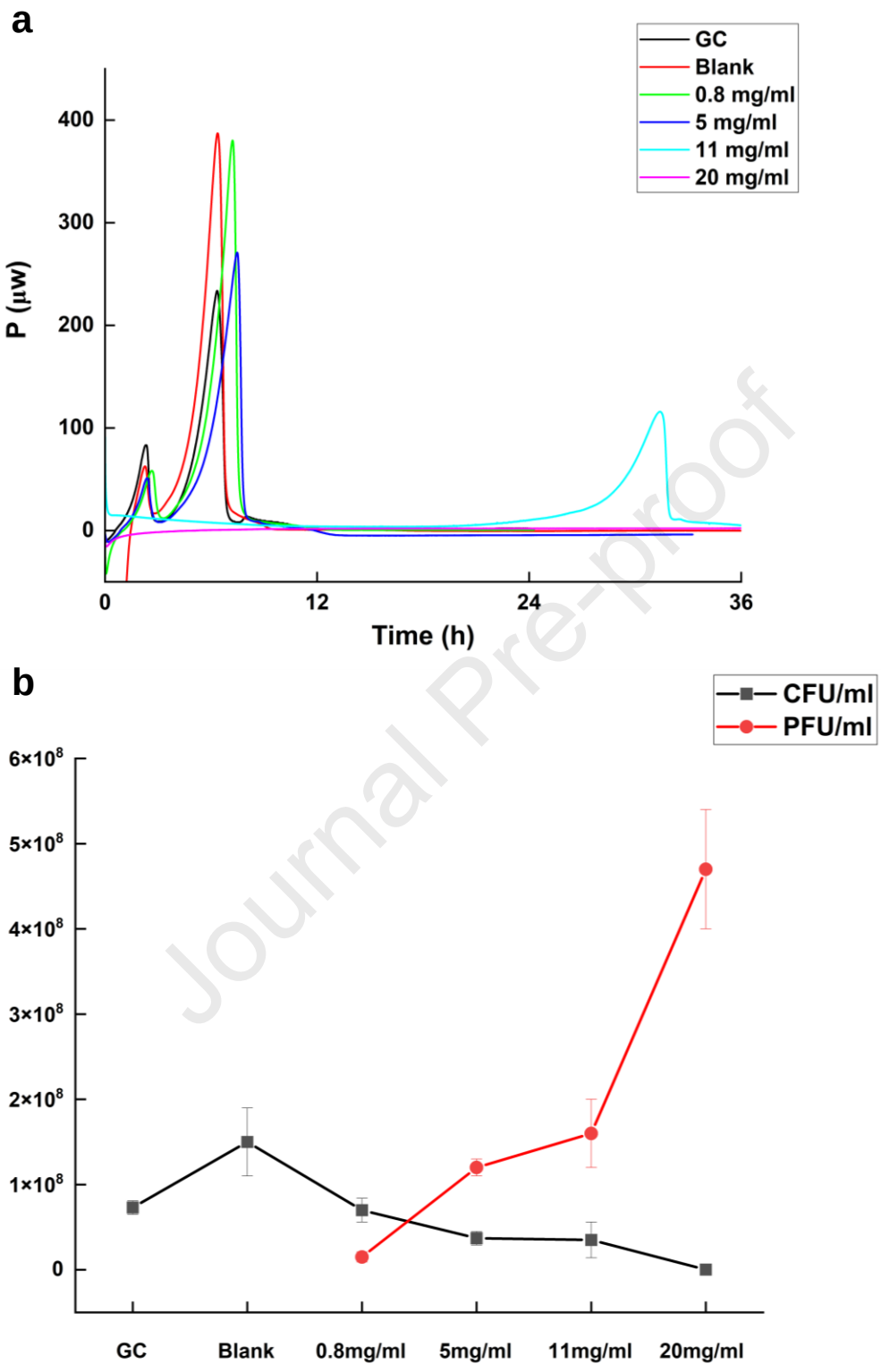

Figure 8 (a) Heat flow (μW) vs time curves of *P. aeruginosa* incubated with the blank formulation (20 mg/ml, 40% w/v solute, LM: PVA=9:1 w/w in SM buffer with 0.1% v/v Triton-X-100) and different concentrations of F_1 (GC: growth

curve). Inoculum of bacteria was 10^6 CFU/ml. **(b)** CFU/ml of *P. aeruginosa,* and phage PFU/ml values obtained with different concentrations of F_1.

3.8 Phage stability

The stability of a batch of phage stock solution stored at RT, 4, and -20 °C was assessed by measuring PFU/ml at different time points (**Figure S7**). -20 °C is found to be the optimal temperature for preserving phages, as it best maintains their activity and count. 4 °C also serves as an effective preservation method but does not result in the same stability as -20 °C. The phages are found to have relatively poor stability under these conditions. This is consistent with previous findings [55]. Though PFU/ml was kept at 10^{10} across all temperatures over 8 weeks, some variability was observed in the data. The fluctuations in phage counts seen across all temperatures (especially at week 4) could be attributed to changes in the aggregation or dispersion of phages in the suspension (the literature reports that phage virions have aggregation/disaggregation transitions [56]). This is consistent with variability reported in the literature for phage stability under different storage conditions [57].

Figure 9 depicts the stability of the same batch of F_1 at RT, 4°C, and -20°C. The PFU/mg of the phage-loaded particles gradually decreases across all temperature conditions, with a more noticeable decline at RT and 4 °C. In contrast, the reduction in phage count is relatively smaller under the -20 °C storage condition, indicating that low temperatures help maintain phage activity. This aligns with findings in the literature [44,58], and with the data obtained on pure phage stocks above. However, it is clear that the particles seem to be less stable than the phage stock solution. Studies have shown a clear hierarchy in the effectiveness of different excipients for maintaining the long-term stability of phage fibers, with SM buffer combined with sugars providing the highest level of protection, followed by SM buffer alone, sugars alone, and finally salts [59,60].

Given that SM buffer is the primary component of the phage stock solution and lactose (a sugar) is the main protective agent in the solid particles, our findings agree with the literature, with somewhat greater stability seen with SM buffer than with the particles. In addition, humidity was not controlled during storage at the three tested temperatures. Especially at 4°C and -20°C, transient condensation likely occurred during sampling, potentially dissolving the water-soluble particles. This could have further disrupted the stability of the encapsulated phages.

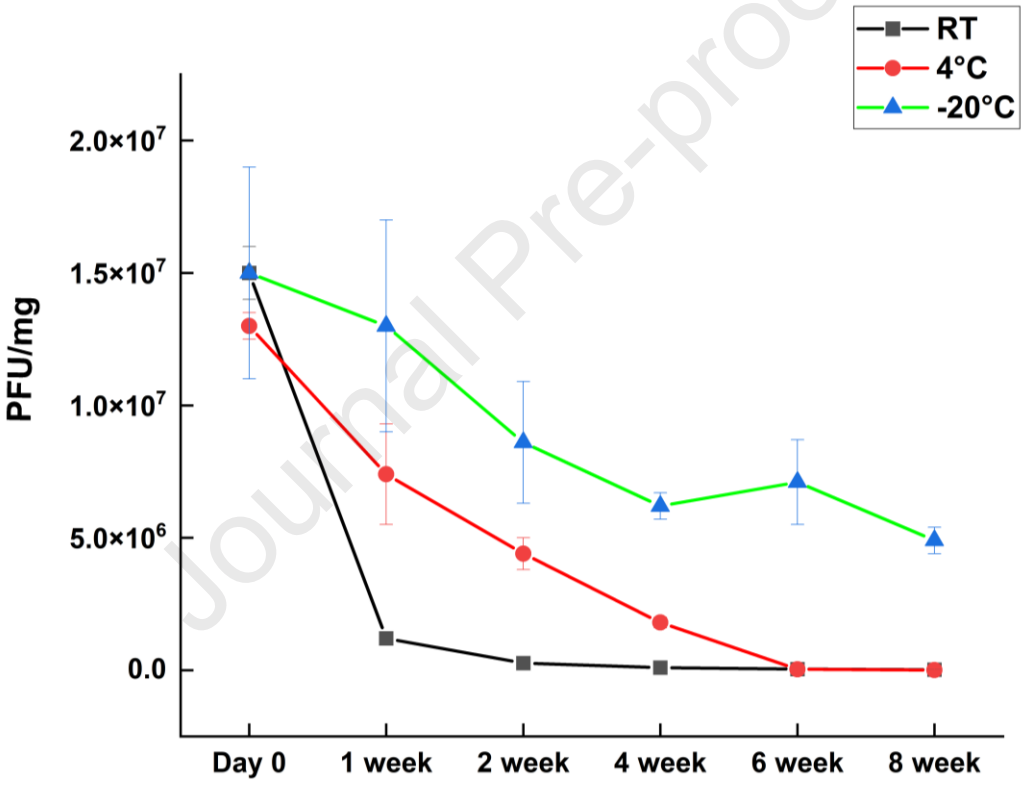

Figure 9 Stability curves of F_1 at RT, 4 °C, and -20 °C over 8 weeks.

In this study, phage-loaded ES lactose particles were developed. To date, these have not been explored for phage formulations. Existing studies have mainly focused on spray-dried lactose-based formulations combined with various excipients to improve phage stability. For example, lactose and leucine have been used in spray-dried phage powders targeting antibiotic-resistant *P.*

aeruginosa (PEV phages) [61], and similar formulations have been developed for different morphotypes of PEV phages as well as PEV20-ciprofloxacin spray-dried powders [62,63]. Additionally, excipients such as trehalose, mannitol, and sucrose have been investigated for their ability to enhance phage stability [62,64-72].

Beyond excipients, storage temperature and relative humidity (RH) are also critical factors influencing the long-term viability of phage powders. Studies have shown that when packaged under dry conditions, spray-dried lactose/leucine phage powders remained biologically and physically stable after being stored at 20°C/60% RH for 12 months [61]. Similarly, spray-dried leucine/trehalose formulations enabled *Podoviridae* and *Myoviridae* phages to be successfully stored under vacuum-sealed conditions at 4°C and 20°C for one year [65]. However, *P. aeruginosa* phage PEV2 powders underwent recrystallization under high humidity conditions (>22% RH), leading to complete phage inactivation after 12 months at 60% RH [66]. Moreover, PEV20-ciprofloxacin powders maintained stability when stored under dry conditions (4°C, 20% RH), whereas storage at 25°C led to a significant decline in phage viability [63]. Exposure to high humidity (65% RH) has been reported to reduce phage recovery due to the recrystallization of amorphous excipients. This effect was observed in *Acinetobacter baumannii* phage vB_AbaM-IME-AB406 formulations [64]. Likewise, spray-dried *P. aeruginosa* phage LUZ19 and *S. aureus* phage Romulus powders exhibited significant recrystallization when exposed to humidity, leading to phage degradation. Moreover, higher storage temperatures (≥25°C) further exacerbated phage instability [69]. Additionally, Eudragit® FS microparticles containing LUZ19 showed substantial activity loss after one month when stored at 25°C, 30°C, or 40°C [71].

In this study, lactose was the main excipient used in the formulation (with PVA added only to enhance solution viscosity and electrosprayability). However,

previous research suggests that spray-dried formulations containing only lactose may provide inadequate protection for phages [67]. This can be attributed to the hygroscopic nature of amorphous lactose, which is thermodynamically unstable and highly susceptible to recrystallization when exposed to moisture. Notably, at a relative humidity of 37%, amorphous lactose has a glass transition temperature (T_g) close to room temperature [73]. Unless both the production and storage conditions are maintained below 37% RH, phage-loaded lactose powders are prone to rapid recrystallization, potentially compromising phage viability.

In this study, only storage temperature was controlled, whereas humidity during both production and storage remained unregulated. This likely contributed to the relatively poor phage stability observed in our electrosprayed formulations. Future studies will focus on improving phage stability by optimizing formulation strategies. Various approaches, including the use of protective excipients, surface coatings, and controlled humidity storage, have been proposed to enhance the long-term viability of phage powders. Our future work will explore these stabilization techniques to improve the practical applicability and shelf life of phage-loaded formulations.

4. Conclusions

This study reports the successful creation of electrosprayable suspensions that ensure phage stability at RT for 24 hours. After electrospraying, phage-loaded particles were successfully generated. By raising the phage stock concentration in the electrospraying feedstock to 50% v/v, the encapsulation efficiency of phages reached 31%, with the phage titer only decreasing from 5×10^7 PFU/mg to 1.5×10^7 PFU/mg, maintaining the same order of magnitude. SEM analysis confirmed the spherical morphology of the particles, while TEM analysis identified phages encapsulated within the particles. The phage-loaded particles

exhibited a burst release within one minute, achieving 99.0 ± 6.9% of phage release within 10 minutes. Although a pure phage stock reduced bacterial numbers, it failed to completely inhibit bacterial growth. Phage-loaded particles demonstrated stronger effects, and at a concentration of 20 mg/ml the particles could completely inhibit bacterial growth over 30 h. A phage suspension remained stable at RT, 4, and -20 °C for eight weeks, with greater stability at lower temperatures. However, for the phage-loaded particles, the PFU/mg gradually decreased across all temperature conditions, with a more noticeable decline at RT and 4°C, indicating that low temperatures are preferred for storage. The observed decline in phage viability is possibly due to the hygroscopic nature of amorphous lactose, which can recrystallize upon exposure to moisture, potentially compromising phage integrity. To address this issue, future work will focus on optimizing excipients, formulations, and storage conditions to enhance phage stability and support the therapeutic potential of electrosprayed phage powders. Nevertheless, our findings offer valuable insights for further developing and optimizing phage-loaded particles as effective antibacterial agents.

References

[1] Azarpazhooh, A. and J.L. Leake, *Systematic review of the association between respiratory diseases and oral health.* Journal of Periodontology, 2006. **77**(9): p. 1465-1482.

[2] Heikkinen, T. and T. Chonmaitree, *Importance of respiratory viruses in acute otitis media.* Clinical Microbiology Reviews, 2003. **16**(2): p. 230-241.

[3] Kim, S.K., et al., *Association Between Pneumonia and Chronic Otitis Media: A Nested Case-Control Study Using a National Health Screening Cohort.* International Journal of Infectious Diseases, 2022. **118**: p. 54-61.

[4] Pichichero, M.E., T.J. Chapman, and P. Bajorski, *Pneumonia, Sinusitis, Influenza and Other Respiratory Illnesses in Acute Otitis Media–Prone Children.* The Pediatric Infectious Disease Journal, 2021. **40**(11): p. 975-980.

[5] Dong, J., et al., *Relationships between oral microecosystem and respiratory diseases.* Frontiers in Molecular Biosciences, 2022. **8**: p. 718222.

[6] Awano, S., et al., *Oral health and mortality risk from pneumonia in the elderly.* Journal of Dental Research, 2008. **87**(4): p. 334-339.

[7] Ahmadi, H., A. Ebrahimi, and F. Ahmadi, *Antibiotic therapy in dentistry.* International Journal of Dentistry, 2021. **2021**(1): p. 6667624.

[8] Sander, R., *Otitis externa: a practical guide to treatment and prevention.* American Family Physician, 2001. **63**(5): p. 927-937.

[9] Frieri, M., K. Kumar, and A. Boutin, *Antibiotic resistance.* Journal of Infection and Public Health, 2017. **10**(4): p. 369-378.

[10] Shlezinger, M., et al., *Phage therapy: a new horizon in the antibacterial treatment of oral pathogens.* Current Topics in Medicinal Chemistry, 2017. **17**(10): p. 1199-1211.

[11] Ryan, E.M., et al., *Recent advances in bacteriophage therapy: how delivery routes, formulation, concentration and timing influence the*

success of phage therapy. Journal of Pharmacy and Pharmacology, 2011. **63**(10): p. 1253-1264.

[12] Sharma, S., et al., *Bacteriophages and its applications: an overview.* Folia Microbiologica, 2017. **62**: p. 17-55.

[13] Abedon, S.T., et al., *Phage treatment of human infections.* Bacteriophage, 2011. **1**(2): p. 66-85.

[14] Olszak, T., et al., *In vitro and in vivo antibacterial activity of environmental bacteriophages against Pseudomonas aeruginosa strains from cystic fibrosis patients.* Applied Microbiology and Biotechnology, 2015. **99**: p. 6021-6033.

[15] Alemayehu, D., et al., *Bacteriophages ϕmr299-2 and ϕnh-4 can eliminate Pseudomonas aeruginosa in the murine lung and on cystic fibrosis lung airway cells.* Mbio, 2012. **3**(2): p. 10.1128/mbio. 00029-12.

[16] Pabary, R., et al., *Antipseudomonal bacteriophage reduces infective burden and inflammatory response in murine lung.* Antimicrobial Agents and Chemotherapy, 2016. **60**(2): p. 744-751.

[17] Debarbieux, L., et al., *Bacteriophages can treat and prevent Pseudomonas aeruginosa lung infections.* The Journal of Infectious Diseases, 2010. **201**(7): p. 1096-1104.

[18] Sulakvelidze, A., Z. Alavidze, and J.G. Morris Jr, *Bacteriophage therapy.* Antimicrobial Agents and Chemotherapy, 2001. **45**(3): p. 649-659.

[19] Sulakvelidze, A. And E. Kutter, *14 bacteriophage therapy in humans.* Bacteriophages: Biology and Applications, 2004. **381**.

[20] Kutter, E., et al., *Phage therapy in clinical practice: treatment of human infections.* Current Pharmaceutical Biotechnology, 2010. **11**(1): p. 69-86.

[21] Burrowes, B., et al., *Bacteriophage therapy: potential uses in the control of antibiotic-resistant pathogens.* Expert Review of Anti-infective Therapy, 2011. **9**(9): p. 775-785.

[22] Mcvay, C.S., M. Velásquez, and J.A. Fralick, *Phage therapy of Pseudomonas aeruginosa infection in a mouse burn wound model.* Antimicrobial Agents and Chemotherapy, 2007. **51**(6): p. 1934-1938.

[23] Fu, W., et al., *Bacteriophage cocktail for the prevention of biofilm formation by Pseudomonas aeruginosa on catheters in an in vitro model system.* Antimicrobial Agents and Chemotherapy, 2010. **54**(1): p. 397-404.

[24] Vandenheuvel, D., R. Lavigne, and H. Brüssow, *Bacteriophage therapy: advances in formulation strategies and human clinical trials.* Annual Review of Virology, 2015. **2**(1): p. 599-618.

[25] Gill, J.J. and P. Hyman, *Phage choice, isolation, and preparation for phage therapy.* Current Pharmaceutical Biotechnology, 2010. **11**(1): p. 2-14.

[26] Emami, F., M. Keihan Shokooh, and S.J. Mostafavi Yazdi, *Recent progress in drying technologies for improving the stability and delivery efficiency of biopharmaceuticals.* Journal of Pharmaceutical Investigation, 2023. **53**(1): p. 35-57.

[27] Zamani, M., M.P. Prabhakaran, and S. Ramakrishna, *Advances in drug delivery via electrospun and electrosprayed nanomaterials.* International Journal of Nanomedicine, 2013: p. 2997-3017.

[28] Tanhaei, A., et al., *Electrospraying as a novel method of particle engineering for drug delivery vehicles.* Journal of Controlled Release, 2021. **330**: p. 851-865.

[29] Bock, N., T.R. Dargaville, and M.A. Woodruff, *Electrospraying of polymers with therapeutic molecules: State of the art.* Progress in Polymer Science, 2012. **37**(11): p. 1510-1551.

[30] Bock, N., et al., *Electrospraying, a reproducible method for production of polymeric microspheres for biomedical applications.* Polymers, 2011. **3**(1): p. 131-149.

[31] Nguyen, D.N., C. Clasen, and G. Van den Mooter, *Pharmaceutical applications of electrospraying.* Journal of Pharmaceutical Sciences, 2016. **105**(9): p. 2601-2620.

[32] Sosnik, A., *Production of drug-loaded polymeric nanoparticles by electrospraying technology.* Journal of Biomedical Nanotechnology, 2014. **10**(9): p. 2200-2217.

[33] Jaworek, A., A. Sobczyk, and A. Krupa, *Electrospray application to powder production and surface coating.* Journal of Aerosol Science, 2018. **125**: p. 57-92.

[34] Sanders, T., A. Milicic, and E. Stride, *Investigating the effect of encapsulation processing parameters on the viability of therapeutic viruses in electrospraying.* Pharmaceutics, 2020. **12**(4): p. 388.

[35] Eninger, R.M., et al., *Electrospray versus nebulization for aerosolization and filter testing with bacteriophage particles.* Aerosol Science and Technology, 2009. **43**(4): p. 298-304.

[36] Jung, J.H., J.E. Lee, and S.S. Kim, *Generation of Nonagglomerated Airborne Bacteriophage Particles Using an Electrospray Technique.* Analytical Chemistry, 2009. **81**(8): p. 2985-2990.

[37] Ergin, F., *Effect of freeze drying, spray drying and electrospraying on the morphological, thermal, and structural properties of powders containing phage Felix O1 and activity of phage Felix O1 during storage.* Powder Technology, 2022. **404**: p. 117516.

[38] Li, Y., et al., *Fabrication of antimicrobial peptide-loaded PLGA/chitosan composite microspheres for long-acting bacterial resistance.* Molecules, 2017. **22**(10): p. 1637.

[39] Park, J.-E., et al., *Biocompatibility and Antibacterial Effect of Ginger Fraction Loaded PLGA Microspheres Fabricated by Coaxial Electrospray.* Materials, 2023. **16**(5): p. 1885.

[40] Ibrahim, A., D. Moodley, and C. Uche, *Antimicrobial and cytotoxic activity of electrosprayed chitosan nanoparticles against endodontic pathogens and Balb/c 3T3 fibroblast cells. Sci Rep 11: 24487*. 2021.

[41] Cecchini, B., et al., *Alginate-based patch for middle ear delivery of probiotics: a preliminary study using electrospray and electrospinning.*

Applied Sciences, 2023. **13**(23): p. 12750.

[42] *Tian Ju, Jixuan Li, Andrew Weston, Giovanni Satta, Sara Bolognini, Mariagrazia Di Luca, Simon Gaisford, and Gareth R. Williams. Anti-Pseudomonas aeruginosa bacteriophage loaded electrospun fibres for antibacterial wound dressings. Macromol. Rapid Comm. 2025, accepted.*

[43] Puapermpoonsiri, U., J. Spencer, and C.F. van der Walle, *A freeze-dried formulation of bacteriophage encapsulated in biodegradable microspheres.* European Journal of Pharmaceutics and Biopharmaceutics, 2009. **72**(1): p. 26-33.

[44] Korehei, R. and J. Kadla, *Incorporation of T4 bacteriophage in electrospun fibres.* Journal of Applied Microbiology, 2013. **114**(5): p. 1425-1434.

[45] Jaworek, A. and A.T. Sobczyk, *Electrospraying route to nanotechnology: An overview.* Journal of Electrostatics, 2008. **66**(3-4): p. 197-219.

[46] Kunisch, F., et al., *Targeting Pseudomonas aeruginosa biofilm with an evolutionary trained bacteriophage cocktail exploiting phage resistance trade-offs.* Nature Communications, 2024. **15**(1): p. 8572.

[47] Braissant, O., et al., *Use of isothermal microcalorimetry to monitor microbial activities.* FEMS Microbiology Letters, 2010. **303**(1): p. 1-8.

[48] Buckton, G., *Applications of isothermal microcalorimetry in the pharmaceutical sciences.* Thermochimica Acta, 1995. **248**: p. 117-129.

[49] von Ah, U., D. Wirz, and A. Daniels, *Isothermal micro calorimetry–a new method for MIC determinations: results for 12 antibiotics and reference strains of E. coli and S. aureus.* BMC Microbiology, 2009. **9**: p. 1-14.

[50] Gaisford, S., et al., *An in vitro method for the quantitative determination of the antimicrobial efficacy of silver-containing wound dressings.* International Journal of Pharmaceutics, 2009. **366**(1-2): p. 111-116.

[51] Carlson, K., *Working with bacteriophages: common techniques and methodological approaches.* Bacteriophages: Biology and Applications, 2005. **1**: p. 437-494.

[52] Chan, B.K., S.T. Abedon, and C. Loc-Carrillo, *Phage cocktails and the*

future of phage therapy. Future Microbiology, 2013. **8**(6): p. 769-783.

[53] Rotman, S.G., et al., *Local bacteriophage delivery for treatment and prevention of bacterial infections.* Frontiers in Microbiology, 2020. **11**: p. 538060.

[54] Liu, P., et al., *Triton X-100 enhanced antibacterial effect of photodynamic therapy against Enterococcus faecalis infection: an in vitro study.* Colloids and Surfaces B: Biointerfaces, 2024. **240**: p. 113978.

[55] Jończyk-Matysiak, E., et al., *Factors determining phage stability/activity: challenges in practical phage application.* Expert Review of Anti-infective Therapy, 2019. **17**(8): p. 583-606.

[56] Szermer-Olearnik, B., et al., *Aggregation/dispersion transitions of T4 phage triggered by environmental ion availability.* Journal of Nanobiotechnology, 2017. **15**: p. 1-15.

[57] Duyvejonck, H., et al., *Evaluation of the stability of bacteriophages in different solutions suitable for the production of magistral preparations in Belgium.* Viruses, 2021. **13**(5): p. 865.

[58] Leung, S.S., et al., *Effect of storage temperature on the stability of spray dried bacteriophage powders.* European Journal of Pharmaceutics and Biopharmaceutics, 2018. **127**: p. 213-222.

[59] Koo, C.K., et al., *Dehydration of bacteriophages in electrospun nanofibers: Effect of excipients in polymeric solutions.* Nanotechnology, 2016. **27**(48): p. 485102.

[60] Dai, M., A. Senecal, and S.R. Nugen, *Electrospun water-soluble polymer nanofibers for the dehydration and storage of sensitive reagents.* Nanotechnology, 2014. **25**(22): p. 225101.

[61] Chang, R.Y.K., et al., *Storage stability of inhalable phage powders containing lactose at ambient conditions.* International Journal of Pharmaceutics, 2019. **560**: p. 11-18.

[62] Chang, R.Y., et al., *Production of highly stable spray dried phage formulations for treatment of Pseudomonas aeruginosa lung infection.*

European Journal of Pharmaceutics and Biopharmaceutics, 2017. **121**: p. 1-13.

[63] Lin, Y., et al., *Storage stability of phage-ciprofloxacin combination powders against Pseudomonas aeruginosa respiratory infections.* International Journal of Pharmaceutics, 2020. **591**: p. 119952.

[64] Yan, W., et al., *The Influence of Formulation Components and Environmental Humidity on Spray-Dried Phage Powders for Treatment of Respiratory Infections Caused by Acinetobacter baumannii.* Pharmaceutics, 2021. **13**(8): p. 1162.

[65] Leung, S.S.Y., et al., *Effect of storage temperature on the stability of spray dried bacteriophage powders.* European Journal of Pharmaceutics and Biopharmaceutics, 2018. **127**: p. 213-222.

[66] Leung, S.S.Y., et al., *Effects of storage conditions on the stability of spray dried, inhalable bacteriophage powders.* International Journal of Pharmaceutics, 2017. **521**(1): p. 141-149.

[67] Vandenheuvel, D., et al., *Feasibility of spray drying bacteriophages into respirable powders to combat pulmonary bacterial infections.* European Journal of Pharmaceutics and Biopharmaceutics, 2013. **84**(3): p. 578-582.

[68] Tabare, E., et al., *A Design of Experiment Approach to Optimize Spray-Dried Powders Containing Pseudomonas aeruginosaPodoviridae and Myoviridae Bacteriophages.* Viruses, 2021. **13**(10): p. 1926.

[69] Vandenheuvel, D., et al., *Instability of bacteriophages in spray-dried trehalose powders is caused by crystallization of the matrix.* International Journal of Pharmaceutics, 2014. **472**(1): p. 202-205.

[70] Carrigy, N.B., et al., *Spray-dried anti-Campylobacter bacteriophage CP30A powder suitable for global distribution without cold chain infrastructure.* International Journal of Pharmaceutics, 2019. **569**: p. 118601.

[71] Tabare, E., et al., *Eudragit® FS Microparticles Containing Bacteriophages, Prepared by Spray-Drying for Oral Administration.* Pharmaceutics, 2023.

15(6): p. 1602.

[72] Zhang, Y., et al., *Manufacturing and ambient stability of shelf freeze dried bacteriophage powder formulations.* International Journal of Pharmaceutics, 2018. **542**(1): p. 1-7.

[73] Roos, Y.H., *Importance of glass transition and water activity to spray drying and stability of dairy powders.* Le Lait, 2002. **82**(4): p. 475-484.

Declaration of Interest Statement

☒ The authors declare that they have no known competing financial interests or personal relationships that could have appeared to influence the work reported in this paper.

☐ The author is an Editorial Board Member/Editor-in-Chief/Associate Editor/Guest Editor for this journal and was not involved in the editorial review or the decision to publish this article.

☐ The authors declare the following financial interests/personal relationships which may be considered as potential competing interests: